Ocular safety of Intravitreal Clindamycin Hydrochloride Released by PLGA Implants

Gabriella M. Fernandes-Cunha, Silvia Ligório Fialho, Gisele Rodrigues da Silva, Armando Silva-Cunha, Min Zhao, Francine Behar-Cohen

Ocular safety of intravitreal clindamycin hydrochloride released by PLGA implants

Gabriella M. Fernandes-Cunha[1,2,3,4*], Silvia Ligório Fialho[5], Gisele Rodrigues da Silva[2,3,4,6], Armando Silva-Cunha[1], Min Zhao[2,3,4] and Francine Behar-Cohen[2,3,4]

[1]Faculty of Pharmacy, Federal University of Minas Gerais, Belo Horizonte, Minas Gerais, Brazil
[2]INSERM UMRS 1138, Team 17, Centre de Recherche des Cordeliers, 75006 Paris, France
[3]Pierre and Marie Curie University, 75005 Paris, France
[4]Paris Descartes University, 75006 Paris, France
[5]Pharmaceutical and Biotechnological Development, Ezequiel Dias Foundation, Belo Horizonte, Minas Gerais, Brazil
[6]Faculty of Pharmacy, Federal University of São João Del Rei, Divinópolis, Minas Gerais, Brazil

*Address for correspondence: Gabriella Maria Fernandes Cunha, Faculty of Pharmacy of the Federal University of Minas Gerais. Av. Presidente Antônio Carlos, 6627. Zip code 31270-901, Belo Horizonte, Minas Gerais, Brazil. Phone: +55-31-34096961; e-mail gabriellafcunha@gmail.com

ABSTRACT

Background

Drug ocular toxicity is a field that requires attention. Clindamycin has been injected intravitreally to treat ocular toxoplasmosis, the most common cause of eye posterior segment infection worldwide. However, little is known about the toxicity of clindamycin to ocular tissues. We have previously showed non intraocular toxicity in rabbit eyes of poly(lactic-co-glycolic acid) (PLGA) implants containing clindamycin hydrochloride (CLH) using only clinical macroscotopic

observation. In this study, we investigated the in vivo biocompatibility of CLH-PLGA implants at microscotopic, cellular and molecular levels.

Methods

Morphology of ARPE-19 and MIO-M1 human retinal cell lines was examined after 72 hours exposure to CLH-PLGA implant. Drug delivery system was also implanted in the vitreous of rat eyes, retinal morphology was evaluated in vivo and ex vivo. Morphology of photoreceptors and inflammation was assessed using immunofluorescence and real-time PCR.

Results

After 72 hours incubation with CLH-PLGA implant, ARPE-19 and MIO-M1 cells preserved the actin filament network and cell morphology. Rat retinas displayed normal lamination structure at 30 days after CLH-PLGA implantation. There was no apoptotic cell and no loss in neuron cells. Cones and rods maintained their normal structure. Microglia/macrophages remained inactive. CLH-PLGA implantation did not induce gene expression of cytokines (IL-1β, TNF-α, IL-6), VEGF, and iNOS at day 30.

Conclusion

These results demonstrated the safety of the implant and highlight this device as a therapeutic alternative for the treatment of ocular toxoplasmosis.

KEY WORDS: Intravitreal implant; Ocular toxoplasmosis; Clindamycin; PLGA; Toxicity; Biocompatibility.

Abbreviations:

PLGA – Poly(lactic-co-glycolic acid)

CLH – Clindamycin hydrochloride

ARPE-19 – Human retinal pigment epithelial cell line

MIO-M1 – Human Müller cell line

IL-1β – Interleukin 1 beta

TNF-α – Tumor necrosis factor alpha

IL-6 – Interleukin 6

VEGF – Vascular endothelial growth factor

iNOS – Inducible nitric oxide synthase

ERG – Electroretinogram

DMEM/F-12 – Dulbecco's modified eagle medium: nutrient mixture F-12

HAM – Human amniotic membrane

HEPES – 4-(2-hydroxyethyl)-1-piperazineethanesulfonic acid

FBS – Fetal bovine serum

PBS – Phosphate-buffered saline

FITC – Fluorescein isothiocyanate

DAPI – 2-(4-amidinophenyl)-1H -indole-6-carboxamidine

IP – Propidium iodide

TUNEL – Terminal deoxynucleotidyl transferase dUTP nick end labeling

PCR – Polymerase chain reaction

OCT – Optical coherence tomography

PNA – Peanut Agglutinin

HPRT – Hypoxanthine phosphoribosyltransferase

SD – Standard deviation

IBA-1 – Ionized calcium binding adaptor molecule 1

OLN – Outer nuclear layer

INL – Inner nuclear layer

GCL – Ganglion cell layer

INTRODUCTION

Drug safety is one of the major concerns in the field of toxicology. When developing a new system for drug delivery, the potential toxicity of both the released drug and the delivery system formulation to the target tissue must be evaluated (1,2). Clindamycin is an antibiotic used to treat infections caused by gram-positive bacteria and has been also suggested to be efficient in the treatment of ocular toxoplasmosis (3-7).

The systemic toxicity of clindamycin is well established (8,9). The oral administration of clindamycin can cause gastrointestinal side effects, such as diarrhea and colitis, which can be life-threatening in severe cases (10). On the other hand, only few reports show the intraocular toxicity of clindamycin. Different studies investigated the retinal toxicity of clindamycin with however controversial results. Vitreous replacement fluid containing 10 µg/mL clindamycin saline has been shown to be non-toxic to the rabbit retina after vitrectomy (Stainer et al., 1977). Abnormal electroretinograms (ERG) and retinal histology were only found in eyes receiving higher drug concentrations (11). In isolated superfused bovine retina, clindamycin at concentration of 0.3 and 1mM (128 and 425 µg/mL) significantly reduced the amplitude of b-wave of ERG, suggesting retinal neural function impairment (12). Lipid intraocular micro-implants (0.4 mm; 5.2 ± 0.5mg) containing clindamycin (50-90%) did not cause retinal abnormalities, inflammatory response nor changes in the b-wave amplitude ratios before and after implantation in rabbit eyes (13). This scenario clearly shows the importance to reevaluate the ocular toxicity of clindamycin.

In previous studies, we have shown that clindamycin hydrochloride (CLH) released by poly(lactic-co-glycolic acid) (PLGA) implants did not cause inflammatory response by clinical evaluation of rabbit eyes, and did not decrease the ARPE-19 cell metabolic activity (14,15). In order to provide more detailed knowledge about the potential ocular toxicity of clindamycin, in the present study, we evaluated the *in vitro* toxicity on retinal cells and *in vivo* drug toxicity in rat

eyes using*in vivo*retinal morphological test by optical coherence tomography, as well as *ex vivo* analyses by histology, immunofluorescence, and real-time PCR. This study, combined with previous reports of the drug anti-parasite activity (15) highlights clindamycin as an alternative treatment for ocular toxoplasmosis.

MATERIALS AND METHODS

Preparation of the CLH-PLGA implants

The implants were developed according to the technique previously described (14-16). CLH (Sigma-Aldrich Co. - St. Louis, MO, USA) and PLGA (50:50 Resomer® RG 503 inherent viscosity midpoint of 0.32-0.44 dl/g – EVONIK, Germany) were dissolved in a mixture of distilled water and acetonitrile and then lyophilized. The resulting mixture was molded into round implants using a hot plate. The final concentration of CLH dispersed in the polymeric system was 25% (w/w) (total amount of the drug was approximately 183.7 µg/implant). This was the maximal drug concentration that maintained PLGA elasticity allowing the implant to be molded. The implants were sterilized by gamma irradiation using cobalt 60 energy source (MDS Nordion, CAN) at room temperature. The dose applied was 15 kGy.

Human cell cultures

Human retinal pigment epithelial (RPE) cells (ARPE-19 cell line) were kindly provided by Dr. Hjelmeland (University of California, Davis, CA) and grow in Dulbecco's modified Eagle's medium (DMEM/F-12) and human amniotic membrane (HAM) nutrient with glutamine, 15mM of HEPES (Life Technologies, Paisfey, UK), and 10% fetal bovine serum (FBS; Invitrogen-Gibco, Grand Island, NY) at 37 °C under 5% CO_2 and 95% humidified air.

Human retinal Muller glial cells (MIO-M1 cell line) were kindly provided by Dr. Astrid Limb, University college London, (London, UK) and grow in the presence of Dulbecco's modified Eagle's medium (DMEM) GlutaMax supplemented (Life Technologies-Gibco, Paisfey, UK) with

10% fetal bovine serum (FBS), 0.4% gemtamicin, and 0.1% amphotericin B in a humidified atmosphere containing 5% CO2, at 37 °C and 95% humidified air.

For both cell cultures, the culture medium was refreshed every 2 days and upon confluence, cells were rinsed with 5 mL of phosphate buffered saline (PBS) and incubated with 10 mL of trypsin-EDTA (Life Technologies) at 37ºC in a humidified atmosphere of 5% CO_2 and 95% humidified air, as previously described (17). After 5 to 10 min, the trypsin enzyme activity was stopped by the addition of 10 mL of the growth medium and the cells were centrifuged for 5 min at 1500 rpm. Then, the supernatant was discarded and the cells were resuspended in 15 mL of fresh respective mediums and seeded into culture flasks for further propagation and subsequent passages.

Immunocellularchemistry

The immunofluorescence study was performed as previously described (18). ARPE-19 and MIO-M1 confluent cells were incubated with culture media alone (no treatment) or containing CLH-PLGA implants or PLGA blank implants. After 72 hours, the media was removed, cells were rinsed with PBS and fixed with paraformaldehyde 4% (v/v) (Merck Eurolab, Fontelay Sous-Bois, France) for 15 min. Cells were then rinsed again with PBS for 5 min and permeabilized in PBS containing 0.3% (v/v) Triton X-100 (Sigma- Aldrich, Lyon, France) for 15 min. F-actin fibers were labeled with FITC-Phalloidin (Sigma-Aldrich) in PBS (1:250) for 30 min at room temperature. Cell nuclei were stained with propidium iodide (IP, 1:100, Sigma-Aldrich) for 30 min or with 4’,6’-diamidino-2-phenylindole (DAPI, 1:5000, Sigma-Aldrich) for 5 min. After washing with PBS, cells were mounted in aqueous mounting medium (Fluoromount, Sigma-Aldrich) and observed using an Olympus IX70 fluorescent microscope equipped with a digital camera.

Animals

All *in vivo* experiments were performed in accordance with the ARVO statement for the Use of Animals in Ophthalmic and Vision Research, the European Communities Council Directive (86/609/EEC), and approved by ethical committees of the Université René Descartes. Adult female Lewis rats (7 weeks old; Janvier, Le Genest-Saint-Isle, France) were kept in pathogen free conditions with food and water and housed in a 12-hour light/12-hour dark cycle.

Implantation of delivery systems into the rat eyes

Prior to the procedure, animals were sedated by intramuscular injection of ketamine (50mg/kg) and xylazine (3mg/kg). Drops of topical anesthetic tetracaine 1% (v/v) (Sigma-Aldrich) were administrated to each eye before the system implantation. Animals were separated in three groups: group I received the CLH-PLGA implant, group II received non-loaded PLGA implant, and group III received no treatment. A transscleral incision was made at 2 mm behind the limbus using 20G needle. The implant was then inserted into the vitreous through the incision (Figure 2C). An experienced surgeon performed the surgical procedure to all animals to assure the reproducibility. After 30 days, rats were killed with a lethal dose of intraperitoneal pentobarbital (Nembutal; Abbot, Saint-Remy sur Avre, France) and eyes were enucleated for histology, immunohistochemistry, TUNEL assay and quantitative PCR. For each analysis, the number of animals is indicated in the respective figure.

Optical Coherent Tomography (OCT)

In vivo assessment of rat retinal morphology was performed immediately and 30 days after polymer implantation using spectral domain OCT (SD-OCT; Spectralis device) as previously described (19). Pupils were dilated with 5% tropicamide drops. Each 2-dimensional B-scan

recorded at 30° field of view consisted of 1,536 A-scans with an optical resolution reaching 3.5 µm, and the enhanced depth imaging option was used to evaluate the choroid and retina.

Histology

Enucleated rat eyes were fixed in 4% (v/v) paraformaldehyde and 0.5% (v/v) glutaraldehyde for 2 hours. Then, the eyes were dehydrated in a graded alcohol series and embedded in historesin (Leica, Heidelberg, Germany). Sections of 5 µm were cut through the optic nerve head using a Leica Jung RM2055 microtome and stained with 1% (v/v) toluidine blue.

Immunohistochemistry on eye cryosections

Eyes were fixed in 4% paraformaldehyde and incubated with a graded series of sucrose before being snap frozen in Tissue-Tek optimal cutting temperature (OCT) compound (Bayer, Diagnostics, Puteaux, France). The following primary antibodies were used on cryosections: rabbit anti-ionized calcium binding adaptor molecule-1 (anti-IBA-1, 1:400; Wako, Richmond, VA, USA), rabbit anti-cone arrestin (1:100; Millipore, Fontenay sous Bois, France), mouse anti-rhodopsin (Rho4D2, 1:100; Abcam, Paris, France). The secondary antibodies (Life Technologies) were Alexa Fluor 488-coupled goat anti-rabbit IgG (1:200), Alexa Fluor 488-coupled goat anti-mouse IgG (1:20) and Alexa Fluor 594-conjugated goat anti-rabbit IgG (1:200). Cone photoreceptor segments were labeled with FITC-conjugated peanut agglutinin (PNA, 1:100; SigmaAldrich). Cell nuclei were stained with DAPI (1:3000; Sigma-Aldrich). Negative controls were performed without primary antibodies. Images were taken using a fluorescence microscope (BX51; Olympus). Cone-arrestin positive cells (cones) and rhodopsin-positive areas of rod outer segments were analyzed using FiJi (ImageJ).

TUNEL assay

For the TUNEL assay, rat eyes were snap frozen in Tissue-Tek OCT-compound (Bayer Diagnostics, Puteaux, France). Cryostat sections (10 µm) were cut and fixed with

methanol/acetic acid for 20 min at room temperature. Then, the sections were rinsed during 10 min in PBS, and permeabilized with 0.1% (w/v) sodium citrate/0.1% (v/v) Triton X-100 in water for 2 min at -4ºC. After that, the sections were rinsed with PBS and incubated for one hour with 50 µL of terminal deoxynucleotidyl transferase (TUNEL; Roche Diagnostics, Mannheim, Germany) reaction mixture at 37 °C. The sections were then rinsed three times with PBS, stained with DAPI and rinsed with PBS.

Reverse transcription and real-time PCR

Total RNA was isolated from neuro-retina and choroid/RPE complex using RNeasy plus Mini Kit (Qiagen, Courtaboeuf, France). First-strand cDNA was synthesized using random primers (Life Technologies). Transcription levels of interleukin 1 (IL-1b), interleukin 6 (IL-6), tumor necrosis factor-α (TNF-α), vascular endothelial growth factor (VEGF) and iNOS were analyzed by Real-Time PCR System (Applied Biosystems, Foster City, CA, USA) with Taqman detection (Life Technologies). The hypoxanthine phosphoribosyltransferase (HPRT) was used as internal control. Delta cycle threshold calculation was used for relative quantification of results.

Statistics

Experimental results were analyzed by two-way ANOVA or Kruskal-Wallis test followed by Dunn's comparasion using GraphPad Prism7 program. A p-value of 0.05 or less was considered statistically significant. Data are presented as mean ± SD.

RESULTS

Human *in vitro* ARPE-19 and MIO-M1 cell morphology after incubation with CLH-PLGA implant. After 72 hours of incubation with CLH-PLGA or PLGA implant, phalloidin-stained actin fibers in ARPE-19 cells were intensely concentrated around the entire perimeter of the cells, suggesting large surface attachment (Figure 1). Highly interconnected cell network was formed

without cytoskeleton lost in both PLGA and CLH-PLGA groups compared to the no treatment group. The actin filaments were distributed in parallel towards circumferential bands. The ARPE-19 cell nuclei stained by DAPI were localized in the center of cytoplasm. Only 3 condensed nuclei were observed. PI is a well-accepted marker for degenerating cells when applied prior to fixation. In fixed tissues, PI staining is able to reveal detailed cell morphology by labeling cell bodies in intact cells, in addition to display condensed nuclei in dead cells (20). In fixed MIO-M1 cells, we observed PI staining in the cytoplasm and nucleoli. No condensed pyknotic nucleus was found in the PLGA or CLH-PLGA group (Figure 1).

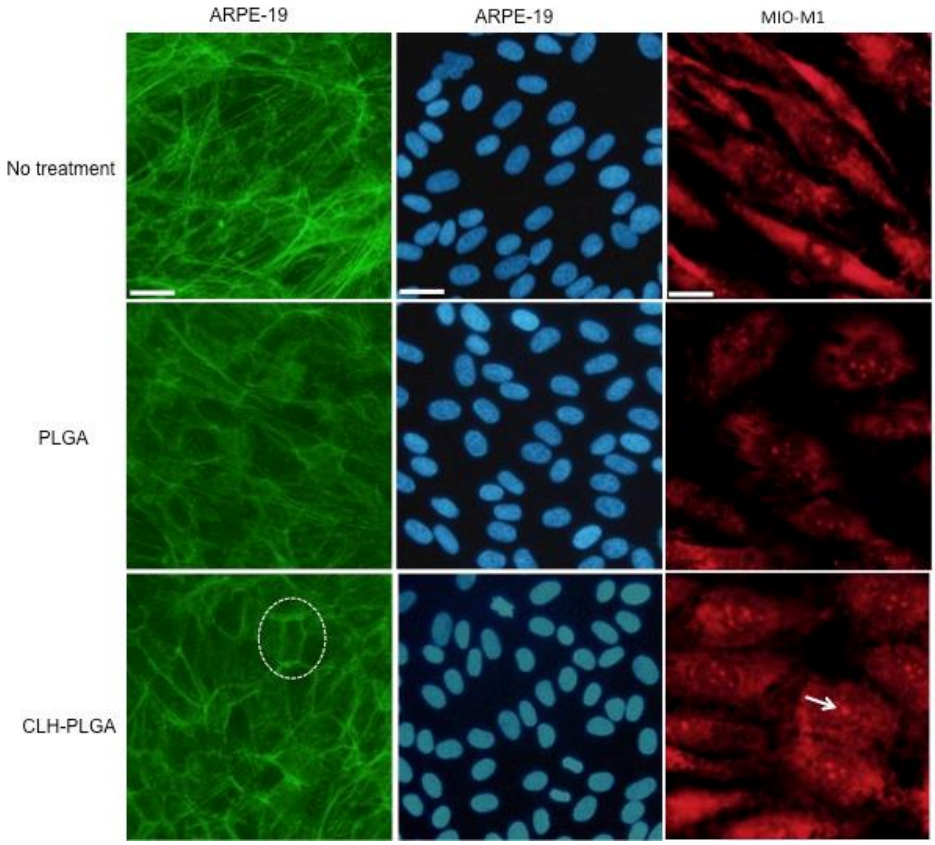

Fig 1. ARPE-19 and MIO-M1 cell morphology after 72 hours of contact with the implants in the different groups. The first column shows the phalloidin-stained actin fibers. The dotted circle shows the actin filament circumferential bands. The second column shows the nuclei stained by DAPI and the third column propidium iodide staining in the cytoplasm and nucleoli. The arrow shows the nucleoli of MIO-M1 cells. All scale bars = 50 µm.

CLH-PLGA implant does not impair retina and photoreceptor morphology and did not induce cell death by apoptosis. The retinal morphology was evaluated *in vivo* by OCT immediately after surgery and 30 days after the system implantation in rat eyes. The OCT shows that the implant was situated in the vitreous (Figure 2). At day 0, the condensed implant was almost dark on OCT as the scanning cannot penetrate it (Figure 2A). At day 30, the implant became hyperreflective suggesting reduced density and degradation of the polymers (Figure 2B). No inflammation or cataract was observed in any animal. Additionally, we didn't observe retinal detachment, retinal edema or thinning, or inflammation (Figure 2D).

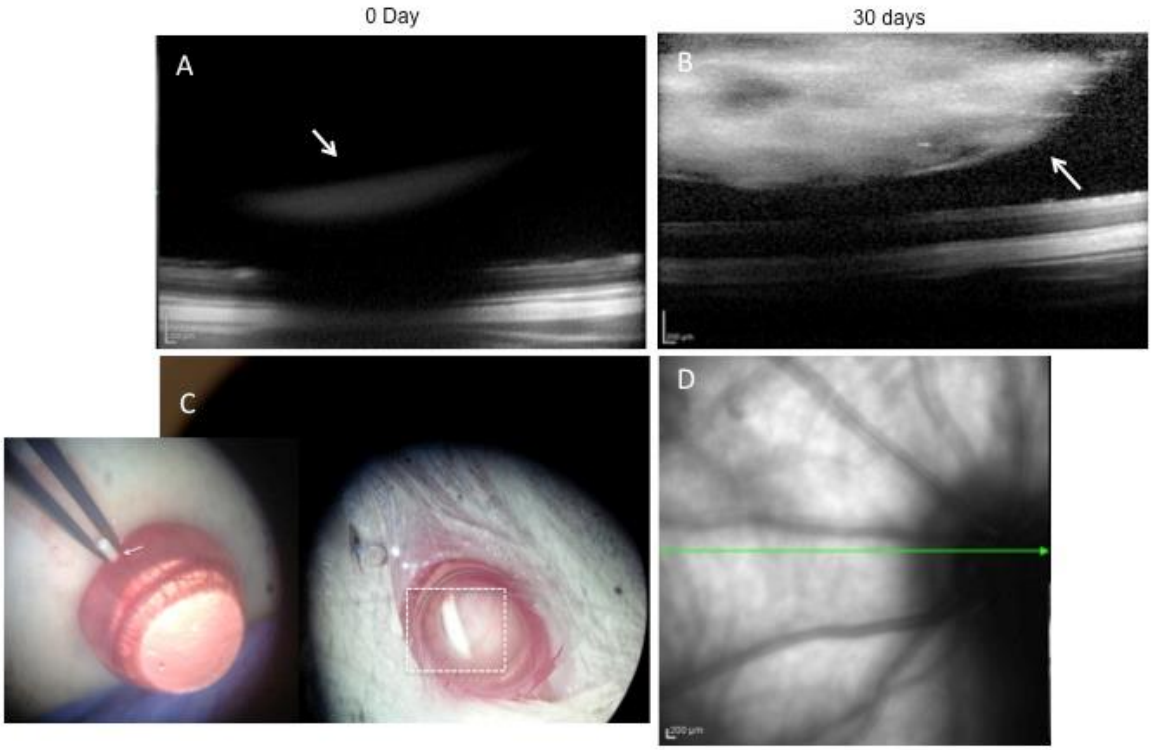

Fig. 2. *In vivo* microscopy and OCT examination of implanted rat eyes. (A) OCT shows that the implant (arrow) is successfully inserted into the vitreous cavity at day 0. The retina is partially masked by the shadow of the implant. The structure of the retina on both sides of the shadow remains normal (B) At day 30, the implant (arrow) becomes hyper-reflective due to its reduced density. The retina below the implant can be observed on the OCT scan. No retinal edema, degeneration of detachment was found. (C) Intraocular CLH-PLGA implant is observed under microscopy. The dotted insert shows the implant inside the rat's eye (D) Retinal fundus shows

normal optic nerve and retinal vasculature at day 30 after polymer implantation. Scale bar = 200 μm, n=3 per group.

On histological sections, the rat retinas in both PLGA- and CLH-PLGA- implanted groups maintained the normal lamination structure at day 30 compared to no treatment group (Figure 3). We didn't observe retinal edema or photoreceptor degeneration, as could happen in toxic conditions (21-23). Furthermore, cell count on the entire retinal section for PLGA- and CLH-PLGA- group showed no significant change compared to no treatment group (Figure 4A).

The outer segments of rods were stained using rhodopsin antibody and cones using cone-arrestin antibody, respectively (Figure 3). No difference was observed in outer segments of rod cells within no treatment, PLGA and CLH-PLGA groups. Cone-arrestin immunestains the entire cone cell from outer segments to synaptic body. No abnormality was observed in cone cell morphology within 3 treatment groups .The rhodopsin and cone-arrestin positive surface area did not decrease compared to no treatment group (Figure 4B).

Apoptosis was assessed by TUNEL assay. We used cornea epithelial cells as positive control (Figure 4C). No apoptotic cell in the rat retinas was observed 30 days after PLGA- or CLH-PLGA- implantation (Figure 4 C and D).

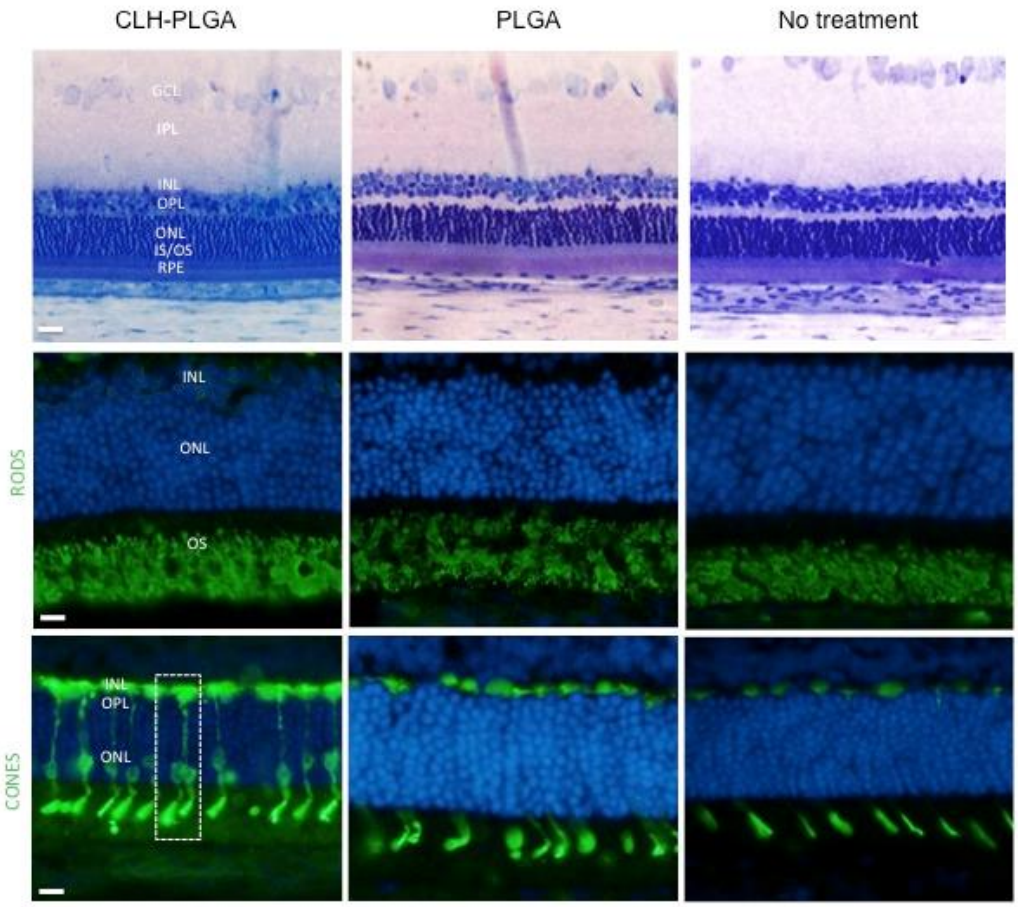

Fig. 3. Ocular biocompatibility of CLH-PLGA implant 30 days after implantation. First row shows toluidine blue stained histological retina sections. Second and third row show rhodopsin staining the outer segments of rod photoreceptors and cone arrestin staining cone photoreceptors. The white dotted line shows the entire cone (outer segments and synaptic bodies). RPE – retinal pigment epithelium; IS/OS – inner and outer segments of photoreceptor; ONL – outer nuclear layer; OPL – outer plexiform layer; INL – inner nuclear layer; IPL – inner plexiform layer; GCL – ganglion cell layer. n = 4 (number of rats per group of immunohistochemistry experiment), n = 3 (number of rats per group of histology experiment) Scale bars: 20 μm.

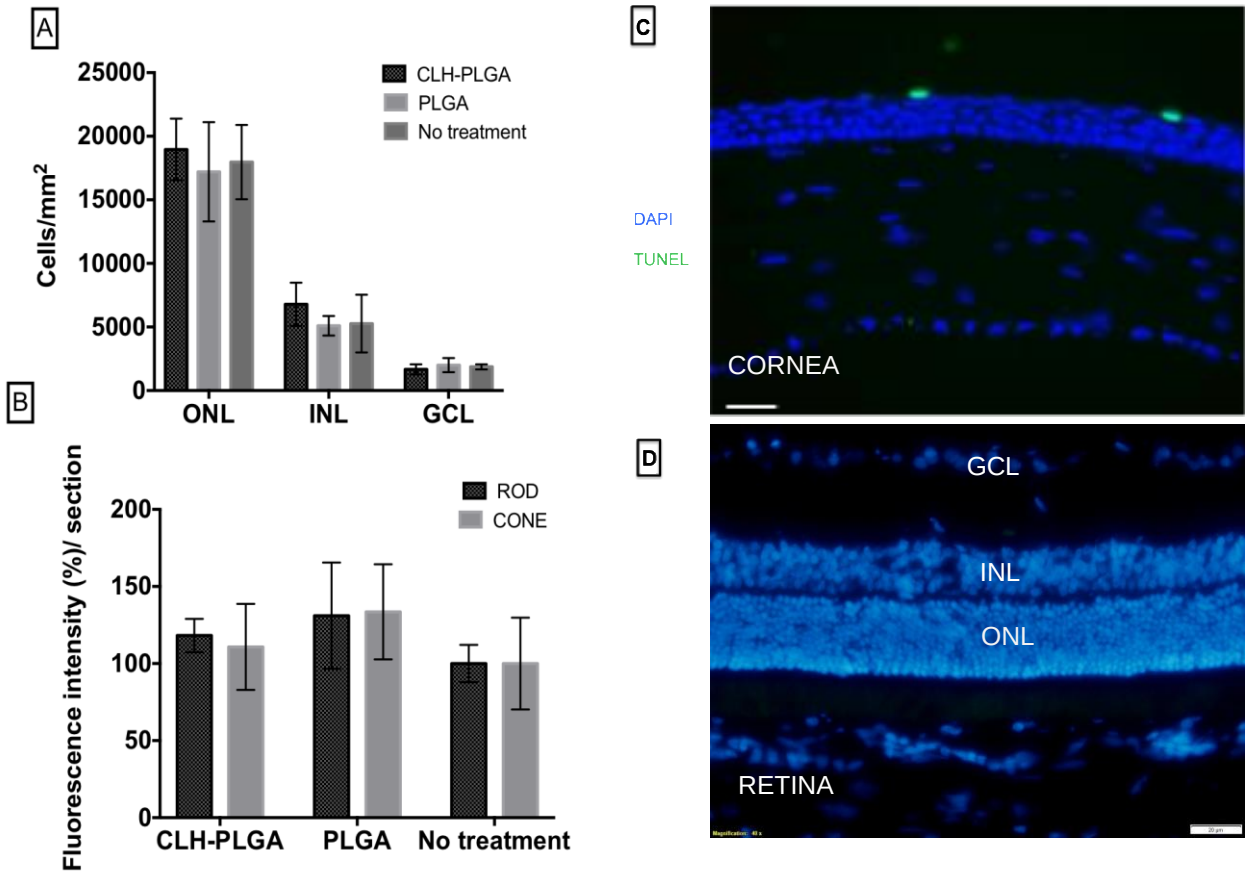

Fig. 4. (A) Cell count of ONL, INL, GCL retina layers and (B) quantification of rhodopsin and cone arrestin positive surface areas by Fiji (ImageJ). (C) Apoptotic corneal epithelial cells (green) are the positive control and nuclei are stained with DAPI (blue). (D) No TUNEL positive cell is observed in the retina of rats. n = 4 rats per group . Scale bars: 50 µm and 20 µm.

CLH-PLGA implant did not induce ocular inflammation. To evaluate whether CLH-PLGA-implant would activate and recruit microglia/macrophage, we performed IBA-1 immunostaining on cryosections. Round-shaped IBA-1 positive microglia/macrophage cells represent activated cells while ramified IBA-1 positive microglia/macrophage cells are resting cells. In the ciliary body of no treatment group, most microglia/macrophageswere inactive (Figure 5 A, yellow arrows), while in the PLGA group, some round-shaped activated microglia/macrophages can be observed (Figure 5 A, white arrows), suggesting acidic PLGA could be somehow inflammatory. In the CLH-PLGA group, microglia/macrophages were mostly inactive. In the retina, ramified

microglia/macrophages were localized in the inner retina in all 3 groups. We did not observe round microglia/macrophages and migration into the outer retina, suggesting no retinal inflammation.

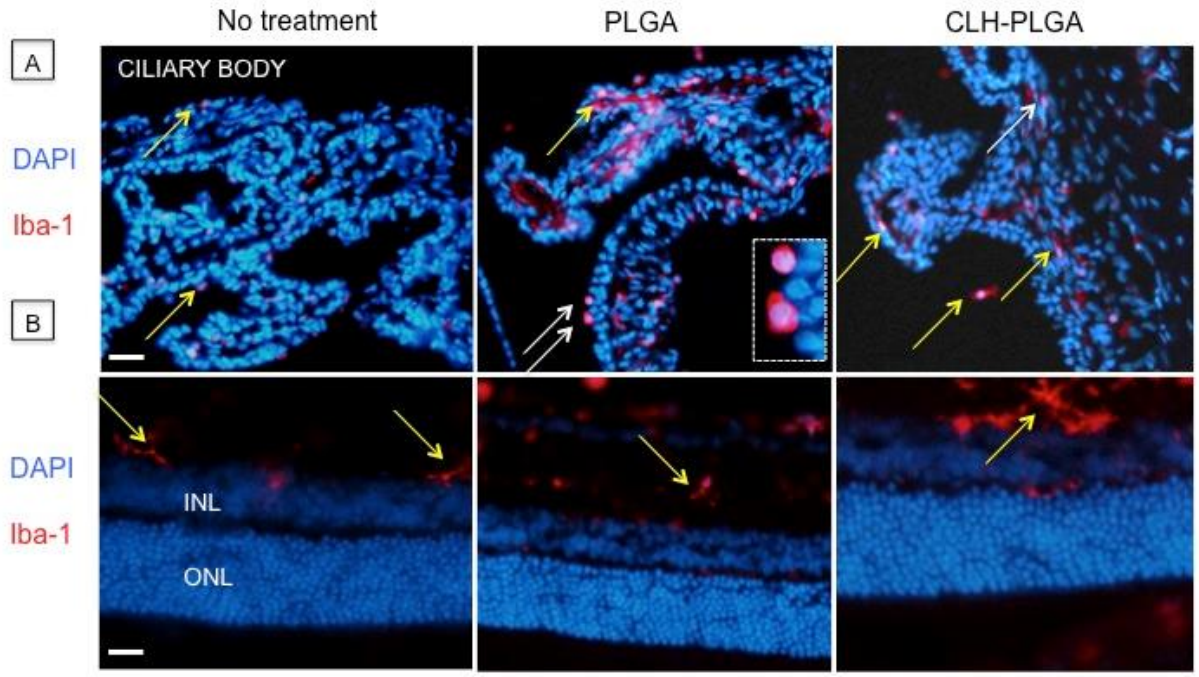

Fig. 5. Microglia activation and expression of pro-inflammatory cytokines in the different groups. (A) IBA-1 immunostaining (red) shows that microglia/macrophages in the ciliary body (anterior segment) display a round shape (white arrows) and resting ramified shape (yellow arrows) (B) The retina stained with IBA-1 shows the absence of activated microglia/macrophages (n = 4 rats per group).

CLH-PLGA implant did not induce gene expression of cytokines. Rat neuroretina and choroid/RPE complex were both analyzed. PCR results showed no significant change in the gene expression of IL-1β, TNF-α, IL-6, iNos and VEGF in groups with system implantation compared to the no treatment group (Figure 6A,B).

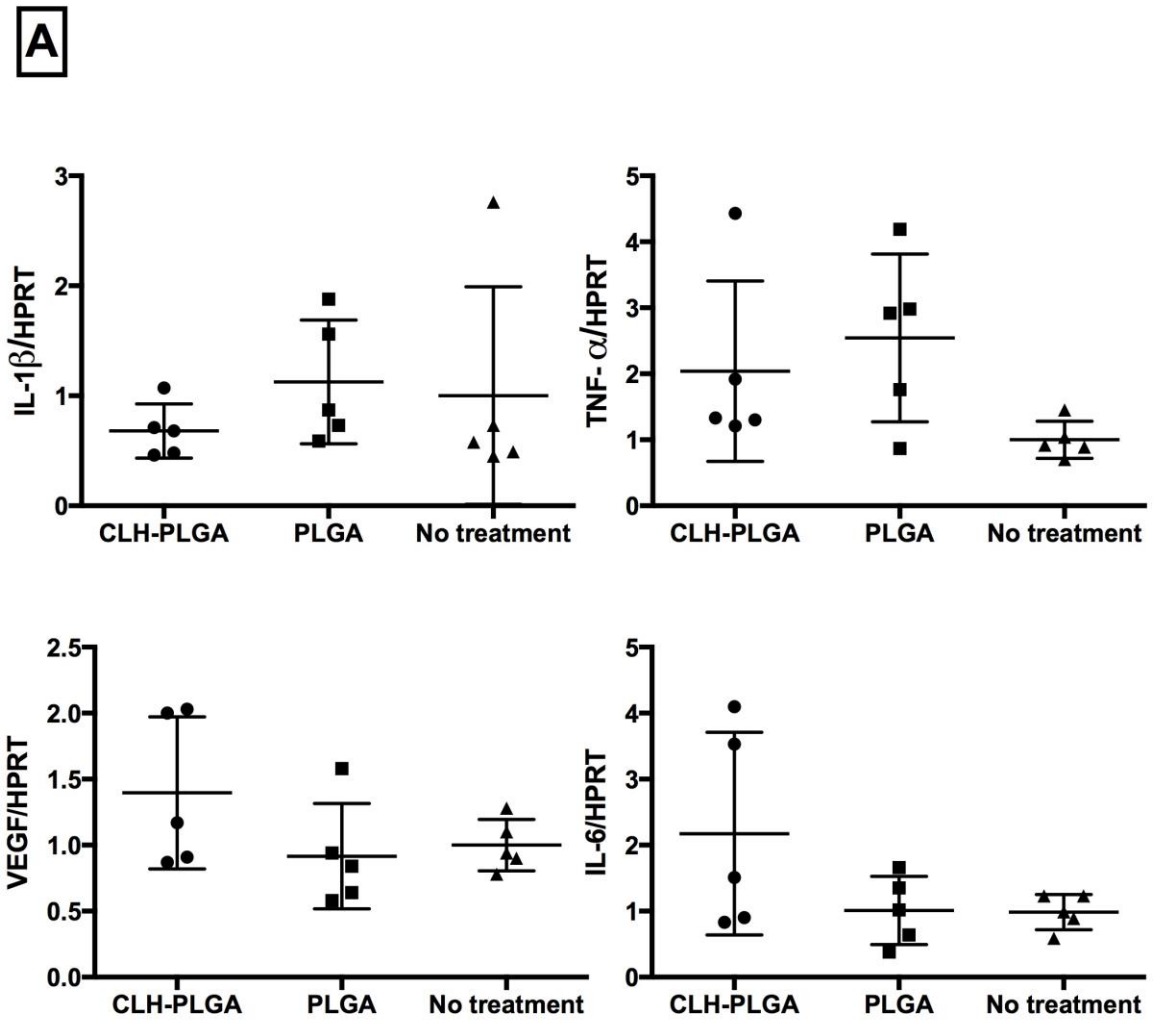
A
IL-1β/HPRT
TNF- α/HPRT
VEGF/HPRT
IL-6/HPRT
CLH-PLGA
PLGA
No treatment

318

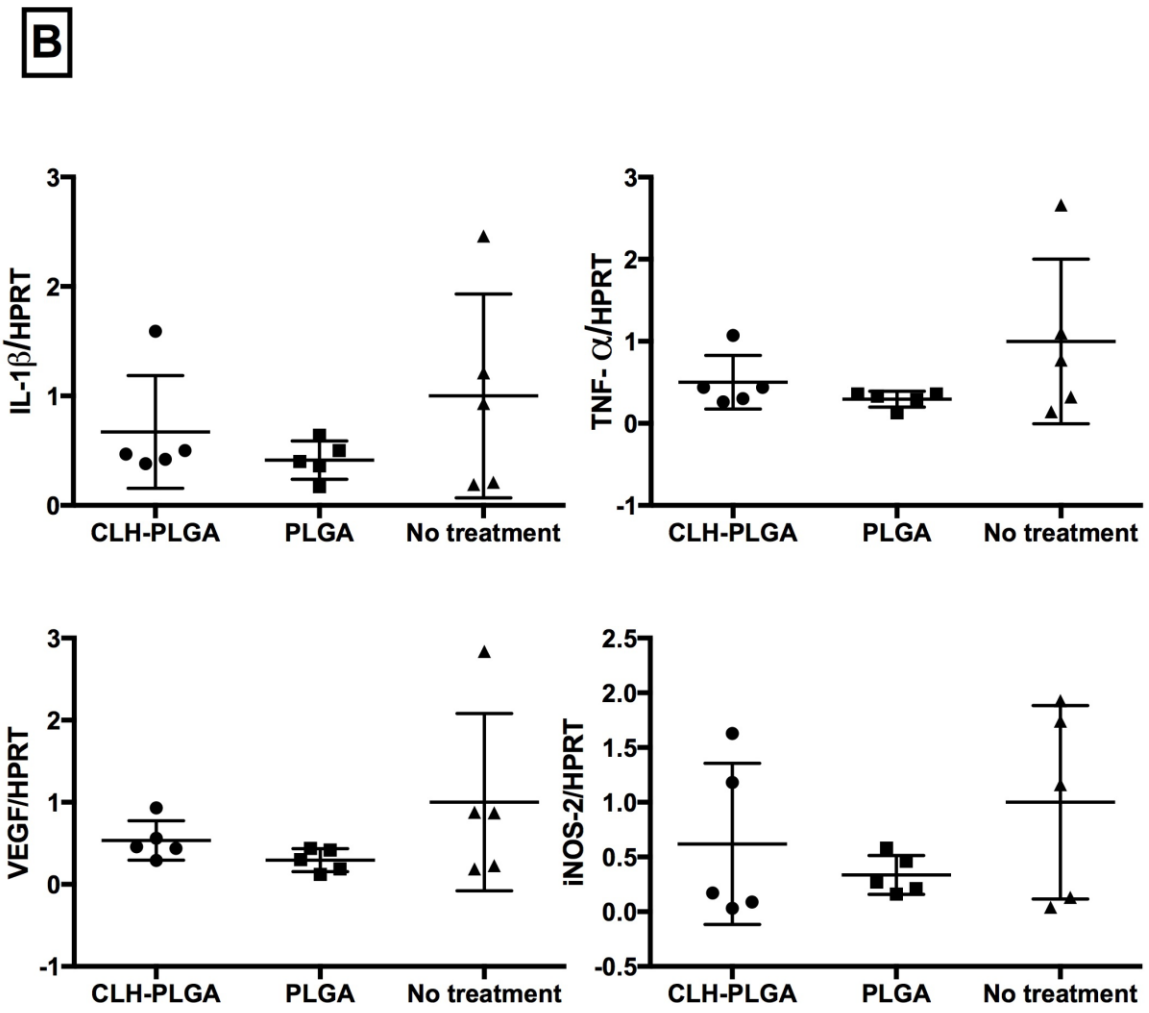

Fig 6. Quantitative PCR of cytokine expression in the retina. HPRT was used as housekeeping gene. Data are expressed relative to the no treatment group (n = 5 rats per group). *P < 0.05.

DISCUSSION

Ocular toxoplasmosis still lacks an effective treatment. Because the ocular bioavailability of drugs administered orally is very low, much effort has been put on local delivery systems. Clindamycin delivery systems have been developed for the treatment of ocular toxoplasmosis or endophthalmitis but the safety of these systems to the retina is not fully evaluated. The interaction between clindamycin and eye tissue has been subject of discussion for several years, but there are no conclusive results. To better understand whether clindamycin is toxic or

not to the eye, here we screened the clindamycin toxicity by in vitro and in vivo studies using a set of techniques. We started by analyzing the *in vitro* cytotoxicity in retinal cells, ARPE-19 and retinal Müller glial cells. The importance to evaluate drug toxicity by using two different retinal cell types has been highlighted (24). Retinal Muller glial cells and RPE both play important role in retinal homeostasis (25,26). Human immortalized ARPE-19 cells are widely used for cytotoxicity studies (27) while Müller cells are major retinal neuron-supporting glial cells. Maintenance of retinal Müller glial homeostasis is essential for the integration of retinal neuronal functions (28). Müller cells have also been used for drug-induced retinal toxicity study (29).

We firstly determine the toxicity of CLH-PLGA/PLGA- implant within 72 hours of incubation with ARPE-19 cells. Actin filaments are responsible to form cell cytoskeleton and therefore alteration in its structure has been considered a potential marker of drug-induced retinal toxicity (30-33). Therefore, we chose to evaluate the morphology of actin filament and cell nuclei as indicators parameter of toxicity. We did not observe any impairment in these structures suggesting that CLH as well as PLGA polymer are not toxic to the ARPE-19 cells. To determine the toxicity of CLH-PLGA- in Müller glial cells (MIO-M1), we used post-fixation PI staining that showed preserved cell morphology after 72 hours incubation with the implant, demonstrating good tolerance. To our knowledge, this is the first cytotoxicity study of CLH using human retinal cell lines.

Our previous study showed the *in vivo* release of CLH from PLGA implant for 6 weeks in rabbit eyes (14). The *in vivo* ocular biocompatibility of the CLH-PLGA has only been evaluated by clinical examination and intraocular pressure measurement (14). In this study, we further assessed the biocompatibility of the implant in rat retinas by *in vivo* and *ex vivo* techniques in order to provide detailed information about the implant safety. Initially, the *in vivo* OCT confirms the stable intravitreous localization of the implant in the rat eyes. After 30 days, the implants decreased in size and density demonstrating its *in vivo* degradation. OCT results did not

evidence any retinal morphological alterations showing the biocompatibility of both the polymer and the drug. In addition to OCT results, histological analysis showed preservation of cell density in the ONL, INL and GCL retinal layers for the CLH-PLGA- implant compared to no treatment group. This suggests that CLH does not provide a toxic environment for the cells. Not surprisingly, TUNEL analysis confirmed the absence of dead cells by apoptosis.

Despite the positive results obtained so far, we wonder whether the photoreceptors maintained their morphology in the presence of the implant. We used immunohistochemistry staining to investigate cone and rod cells. No abnormality was found in the morphology of both photoreceptors suggesting no neurodegeneration.

Chronic inflammation and activation of microglia can lead to retinal damage and neuronal apoptosis (34). At 30 days after intravitreous implantation of PLGA system, there was no microglia/microphage activation and migration compared to no treatment groups. However, some activated microglia/macrophages were observed in the ciliary body in rats implanted with non-loaded PLGA. The degradation products of PLGA, lactic and glycolic acid, are known to be inflammatory. As CLH-PLGA did not induce activation of microglia/macrophages, whether antibiotic clindamycin inhibits PLGA induced inflammation should be further investigated. Real-time PCR showed no significant changes in gene expression of cytokines and VEGF, confirming the ocular tolerance of the CLH-PLGA systems.

Our study provides evidences of ocular safety of clindamycin released PLGA system by combining in vitro and in vivo evaluations. PLGA implant allows continuous release of minimal therapeutic dose of CLH, improving retinal biocompatibility. This CLH delivery system could be a therapeutic alternative for the treatment of ocular toxoplasmosis.

CONCLUSION

In this study, we evaluated *in vitro* toxicity of clindamycin released from PLGA implants using 2 human retinal cell lines and biocompatibility of PLGA containing CLH in rat eyes using *in vivo* OCT examination, histology, TUNEL assay, immunohistochemistry and real-time PCR. *In vitro*tests on retinal cells showed the preservation of ARPE-19 and MIO-M1 cell morphology after 72 hours incubation with CLH-PLGA implant. *In vivo* biocompatibility showed normal retinal and photoreceptor morphology, absence of apoptotic cells and inflammation 30 days after CLH-PLGA implantation, suggesting good ocular biocompatibility. PLGA implant containing CLH could be proposed as a therapeutic alternative for the treatment of ocular toxoplasmosis.

ACKNOWLEDGEMENTS

The authors would like to acknowledge the financial support received from the following institutions: (Brazil), FAPEMIG (Minas Gerais – Brazil), Pró-reitoria de Pesquisa da Universidade Federal de Minas Gerais (Minas Gerais – Brazil), CAPES (Bolsistas da CAPES-Brasília/Brazil).

REFERENCES

1.SalibaJB, Vieira L, Fernandes-Cunha GM, Silva GR, Fialho SL, Silva-Cunha A, Bousquet E, Naud MC, Ayres E, OréficeRL, Tekaya M, Kowalczuk L, Zhao M, Behar-Cohen F. Anti-Inflammatory Effect of Dexamethasone Controlled Released From Anterior Suprachoroidal Polyurethane Implants on Endotoxin-Induced Uveitis in Rats. Invest. Ophthalmol. Vis. Sci. 57(4):1671-1679, 2016

2.Elsaesser A, Howard CV. Toxicology of nanoparticles. Advanced Drug Delivery Reviews 64(2): 129–137, 2012.

3.Peyman GA, Charles HC, Liu KR, Khoobehi B, Niesman M. Intravitreal liposome-encapsulated drugs: a preliminary human report. IntOphthalmol 12:175-182, 1988.

4.Kishore K et al. Intravitreal clindamycin and dexamethasone for toxoplasmic retinochoroiditis. Ophthalmic Surg Lasers 32:183-192, 2001.

5.Sobrin L, Kump LI, Foster CS. Intravitreal clindamycin for toxoplasmic retinochoroiditis. Retina 27:952-957, 2007.

6.Lasave AF, Díaz-Llopis M, Muccioli C, Belfort R, Arevalo JF. Intravitreal clindamycin and dexamethasone for zone 1 toxoplasmic retinochoroiditis at 24 months. Ophthalmology 117:1831-1838, 2010.

7. Soheilian M, Ramezani A, Azimzadeh A, Sadoughi MM, Dehghan MH, Shahghdami R, Yaseri M, Peyman GA. Randomized trial of intravitreal clindamycin and dexamethasone versus pyrimethamine, sulfadiazine, and prednisolone in treatment of ocular toxoplasmosis. Ophthalmology 118:134-141, 2011.

8.Tabbara KF, O'Connor GR. Treatment of ocular toxoplasmosis with clin- damycin and sulfadiazine. Ophthalmology 87:129-134,1980.

9.Maenz M, Schlüter D, Liesenfeld O, Schares G, Gross U, Pleyer A. Ocular toxoplasmosis past, present and new aspects of an old disease. Progress in Retinal and Eye Research, 39:77-106, 2014.

10.Neu HC, Pnnce A, Neu CO, Garvey GJ. Incidence of diarrhea and colitis associated with clindamycim therapy. Infect DIs 135:120-125,1977.

11.Stainer GA, Peyman GA, Meisels H, Fishman G. Toxicity of selected antibiotics in vitreous replacement fluid. Ann Ophthalmol 9(5):615-618, 1977.

12.Walter P, Lüke C, Sickel W. Antibiotics and Light Responses in Superfused Bovine Retina. Cellular and Molecular Neurobiology 19(1):87-92, 1999.

13.Tamaddon L, Mostafavi A, Riazi-esfahani M, Karkhane R, Aghazadeh S, Rafiee-Tehrani M, Dorkoosh FA, Amoli FA. Development, Characterizations and Biocompatibility Evaluations of Intravitreal Lipid Implants. Jundishapur J Nat Pharm Prod 9(2): e16414, 2014.

14.Fernandes-Cunha GM, Gouvea DR, Fulgêncio GO, Rezende CMF, Da Silva GR, Bretas JM, Fialho SL, Lopes NP, Silva-Cunha A. Development of a method to quantify clindamycin in vitreous humor of rabbits' eyes by UPLC–MS/MS: Application to a comparative pharmacokinetic study and in vivo ocular biocompatibility evaluation. Journal of Pharmaceutical and Biomedical Analysis 102:346-352, 2015.

15. Fernandes-Cunha GM, Rezende CMF, Mussel WN, Da Silva GR, Gomes ECL, Yoshida MI, Fialho SL, Goes AM, Gomes DA, Almeida-Vitor RW, Silva-Cunha, A. Anti-Toxoplasma activity and impact evaluation of lyophilization, hot molding process, and gamma-irradiation techniques on CLH-PLGA intravitreal implants. Journal of Materials Science: Materials in Medicine 27(10) doi:10.1007/s10856-015-5621-1, 2016.

16.Fialho SL, Silva-Cunha A. Manufacturing techniques of biodegradable implants intended for intraocular application. Drug Deliv 12(2):109–116,2005.

17.Da Silva GR, Lima TH, Oréfice RL, Fernandes-Cunha GM, Silva-Cunha A, Zhao M, Behar-Cohen F. In vitro and in vivo ocular biocompatibility of electrospun poly(e-caprolactone) nanofibers. European Journal of Pharmaceutical Sciences 73:9–19, 2015.

18.Zhao M, Valamanesh F, Celerier I, Savoldelli M, Jonet L, Jeanny JC, Jaisser F Farman N, Behar-Cohen F. The neuroretina is a novel mineralocorticoid target: aldosterone up-regulates ion and water channels in Muller glial cells. The FASEB Journal 24, 3405–3415, 2010.

19.Zhao M, Célérier I, Bousquet E, Jeanny JC, Jonet L, Savoldelli M, Offret O, Curan A, Farman N, Jaisser F, Behar-Cohen F. Mineralocorticoid receptor is involved in rat and human ocular chorioretinopathy. The Journal of Clinical Investigation 122 (7): 2672-2679, 2012.

20.Hezel M, Ebrahimi F, Kocha M, Dehghani F. Propidium iodide staining: A new application in fluorescence microscopy for analysis of cytoarchitecture in adult and developing rodent brain. Micron 43:1031–1038, 2012.

21.Brock WJ, Somps CJ, Torti V, Render JA , Jamison J, Rivera MI. Ocular Toxicity Assessment From Systemically Administered Xenobiotics: Considerations in Drug Development. International Journal of Toxicology 32(3) 171-188, 2013.

22.Söderstjerna E, Bauer P, Cedervall T, Abdshill H, Johansson F, Johansson UE. Silver and Gold Nanoparticles Exposure to In Vitro Cultured Retina – Studies on Nanoparticle Internalization, Apoptosis, Oxidative Stress, Glial- and Microglial Activity. Plos One 9(8): e105359, 2014.

23.Siqueira RC, dos Santos WF, Scott IU, Messias A, Rosa MN, Fernandes Cunha, GM, Silva-Cunha A, Jorge R. Neuroprotective effects of intravitreal triamcinolone acetonide and dexamethasone implant in rabbit retinas after pars plana vitrectomy and silicone oil injection. Retina 0:1-7,2014.

24.Penha FM, Rodrigues EB, Maia M, Dib E, Fiod Costa E, Furlani BA, NunesMoraesFilho M, Dreyfuss JL, Bottós J, Farah ME. Retinal and ocular toxicity in ocular application of drugs and chemicals--part I: animal models and toxicity assays. Ophthalmic Research 44(2):82-104, 2010.

25.Bringmann A; Pannicke T, Grosche J, Francke M, Wiedemann P, Skatchkov SN, Osborne NN, Reichenbach A. Müller cells in the healthy and diseased retina. Prog Retin Eye Res 25:397-424, 2006.

26.Chiba C. The retinal pigment epithelium: an important player of retinal disorders and regeneration. Exp Eye Res 123:107-114, 2014.

27. Luo Y, Zhuo Y, Fukuhara M, Rizzolo LJ. Effects of Culture Conditions on Heterogeneity and the Apical Junctional Complex of the ARPE-19 Cell Line. Investigative Ophthalmology & Visual Science 47(8):3644-3655,2006.

28.Dubois-Dauphin M, Poitry-Yamate C, de Bilbao F, Julliard A, Jourdan F, DonatiG.Early postnatal Müller cell death leads to retinal but not optic nerve degeneration in transgenic mice. Neuroscience 95:9-21,2000.

29.Ramadan GA. Sorbitol-Induced Diabetic-Like Retinal Lesions in Rats: Microscopic Study. American Journal of Pharmacology and Toxicology 2(2): 89-97, 2007.

30. Maddala R, Reddy VN, Epstein DL, Rao V: Growth fator induced activation of Rho and RacGTPases and actin cytoskeletal reorganization in human lens epithelial cells. Mol Vis 9:329–336, 2003.

31.Hall A: Rho GTPases and the actin cytoskeleton. Science 279:509–514, 1998.

32.Winkler J, Hagelstein S, Rohde M, Laqua H: Cellular and cytoskeletal dynamics within organ cultures of porcine neuroretina. Exp Eye Res 74:777–788, 2002.

33.Verdugo-Gazdik ME, Simic D, Opsahl AC, Tengowski MW. Investigating cytoskeletal alterations as a potential marker of retinal and lens drug-related toxicity. Assay Drug Dev Technol 4(6):695-707, 2006.

34.Ebert S, Schoeberl T, Walczak Y, Stoecker K, Stempfl T, Moehle C, Weber BHF,Langmann T. Chondroitin sulfate disaccharide stimulates microglia to adopt a novel regulatory phenotype. J Leukoc Biol. 84(3):736-40, 2008.